Chin.J.Geochem.(2013)32:157–169
DOI: 10.1007/s11631-013-0618-2

The generation kinetics of natural gases in the Kela-2 gas field from the Kuqa Depression, Tarim Basin, northwestern China

LI Xianqing[1, 2*], FENG Songbao[1], XIAO Xianming[2], TANG Yongchun[3], XIAO Zhongyao[4], MI Jingkui[5], TIAN Hui[2], LIU Dehan[2], and SHEN Jiagui[2]

[1] *State Key Laboratory of Coal Resources and Safe Mining, China University of Mining and Technology, Beijing 100083, China*

[2] *State Key Laboratory of Organic Geochemistry, Guangzhou Institute of Geochemistry, Chinese Academy of Sciences, Guangzhou 510640, China*

[3] *Power, Environmental and Energy Research Center, California Institute of Technology, 738 Arrow Grand Circle, Covina, California 91722, USA*

[4] *Research Institute of Exploration and Development, Tarim Oilfield Company, PetroChina, Korla 841000, China*

[5] *Research Institute of Petroleum Exploration and Development, PetroChina, Beijing 100083, China*

* *Corresponding author, E-mail: Lixq@cumtb.edu.cn*

Received February 15, 2012; accepted March 10, 2012

Abstract The Kela-2 gas field, found in the Kuqa Depression of the Tarim Basin, northwestern China, is a large-sized dry gas field (C_1/C_{1-5}=0.992−0.999) and characterized by ultra-high pressure (pressure factor up to 2.0−2.2). The pyrolysis experiment was carried out under isothermal gold-tube closed system, with samples collected from the Jurassic coal, Jurassic mudstone and Triassic mudstone in the Kuqa Depression. The result of gas yield showed that the Middle and Lower Jurassic source rocks have higher gas generation potential than the Triassic source rocks. The kinetic modeling of gas generation and methane carbon isotope fractionation suggested that the Kela-2 gases belong to the products of high-over mature stages and were mainly derived from the Middle and Lower Jurassic coal-bearing strata. The Triassic source rocks made a minor contribution to the Kela-2 gases. The Kela-2 gases chiefly generated from coal-bearing source rocks with R_o values from 1.3% to 2.5%, and thus primarily accumulated after 5 Ma.

Key words natural gas; pyrolysis experiment; gas generation kinetics; carbon isotope fractionation; Kela-2 gas field

1 Introduction

As natural gases are dominated by a few simple, low molecular weight hydrocarbons, important genetic information is commonly developed from the chemical components and stable carbon isotopic ratios, which can be used to assess the nature and thermal maturity of potential source beds of natural gases (Stahl et al., 1975; Stahl, 1977; Schoell, 1980, 1983; Whiticar et al., 1986; Dai Jinxing et al., 1992; Xu Yongchang et al., 1994). On the basis of gas component and isotope data from different basins, a lot of empirical relationships between carbon isotopic values of C_1-C_4 hydrocarbons and the vitrinite reflectance (R_o) of source rocks have been established (Stahl et al., 1975; Stahl, 1977; Faber et al., 1987; Shen Ping et al., 1988; Dai Jinxing et al., 1989, 1992; Clayton, 1991; Xu Yongchang et al., 1994). However, the empirical relationships obtained from one basin often do not work for another, sometimes even lead to a contradictory conclusion (Jenden et al., 1993; Lorant et al., 1998; Li Xianqing, 2004; Li Xianqing et al., 2003, 2005, 2008), and a given data set may give rise to different interpretations, particularly when post-generation processes are invoked (Prinzhofer et al., 1995, 1997).

With the above interpretive principles being derived from field data, pyrolysis and chemical kinetic modeling play an important role in constraining the origin, migration and accumulation of natural gases, as well as the maturity of source rocks (Berner et al., 1995; Tang et al., 2000; Cramer et al., 1998, 2001; Li

Xianqing et al., 2005). Attempts have been made to obtain the kinetic parameters for oil and gas generation through thermal cracking of kerogen using laboratory pyrolysis experiments (e.g., Behar et al., 1991, 1997; Burnham et al., 1989). Some kinetic models have been developed to describe and predict variations in $\delta^{13}C$ values of C_1-C_4 gaseous hydrocarbons during natural gas formation (Galimov, 1988; Berner et al., 1992, 1995; Rooney et al., 1995; Lorant et al., 1998; Tang et al., 2000; Cramer et al., 1998, 2001; Li Xianqing et al., 2003, 2004, 2005, 2008). The results showed how carbon isotopic compositions can be related to gas generation rates, net gas yields and reservoir accumulation histories. These models are of great value in natural gas assessment and exploration because they can be combined with sedimentary and burial histories and paleoheat flow reconstructions to make useful predictions about the distribution of hydrocarbons in sedimentary basins.

The Kela-2 gas field is located in the east of the Kelasu tectonic zone in the Kuqa Depression of the Tarim Basin, northwestern China. The present exploration shows that its reserve is more than 2500×10^8 m^3. As its area is less than 50 km^2, natural gases are much more richly accumulated in this gas field. Since its discovery, the Kela-2 gas field has attracted great attention in China (Qin Shengfei, 1999; Jia Chengzhao et al., 2000; Dai Jinxing et al., 2000; Liang Digang et al., 2002, 2003; Zhao Mengjun et al., 2002; Zhang Qiming, 2002; Li Xianqing et al., 2005, 2008). It is really significant both theoretically and practically in studying the generation and accumulation of the Kela-2 gases. Moreover, it also can be a useful reference in the study of other oil and gas fields in the Tarim Basin.

2 Geological setting and characteristics of the Kela-2 gases

The Tarim Basin, located in northwestern China, is a giant basin that has not been fully explored. Geographically, the Tarim Basin is surrounded by the Tianshan Mountains to the north, and the Kulun Mountains and Altun Mountains to the south. The basin is filled with sedimentary rocks ranging in age from Sinian to Quaternary with the maximum thickness up to 15000 m. Recent advances in exploration show that the Tarim Basin is very abundant in oil and gas resources (Jia Chengzhao et al., 2000; Liang Digang et al., 2002, 2003).

The Kuqa Depression is located in the northern part of the Tarim Basin near southern Tianshan Mountains. It is divided into four belts and two sags, i.e. northern Monocline Belt, Kelasu Anticline Belt, Baicheng Sag, Yangxia Sag, Qiulitake Anticline Belt, and southern Anticline Belt (Fig. 1).

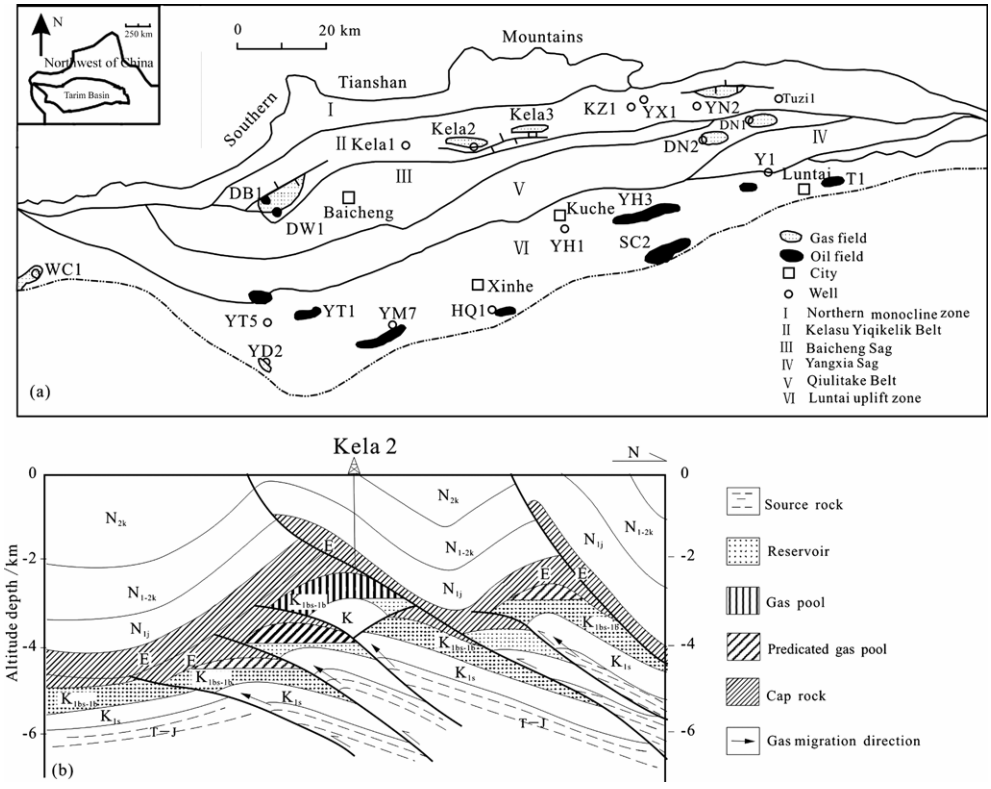

Fig. 1. Sketch map showing the tectonic units and the distribution of oil and gas fields in the Kuqa Depression of the Tarim Basin (a); the cross-section of the Kela-2 gas field (b).

The Kuqa Depression is a Cenozoic foreland basin where the Mesozoic-Cenozoic terrestrial sedimentary rocks are up to 12000 m thick in the sedimentary center. As shown in Fig. 2, in the Mesozoic strata, there are Triassic-Jurassic source rocks (such as coal, carbonaceous mudstone and dark mudstone) at the lower part and giant thick (>8000 m) Cretaceous and Tertiary terrestrial deposits in the middle-upper part (Dai Jinxing et al., 2000; Liang Digang et al., 2002). Several sets of assemblages of reservoir rocks and seal rocks are found in the Kuqa Depression. The Cretaceous and Paleogene sandstones are the main reservoir rocks while the Triassic and Lower Jurassic sandstones are other reservoir rocks (Gu Jiayu et al., 2002). The regional seal rocks are mainly mudstone, coal, and gypsum-bearing mudstone. There are the Upper Jurassic mudstone, Lower and Middle Jurassic coal-bearing strata, Tertiary gypsum-bearing mudstone and salt rocks. Especially the Tertiary gypsum salt and mudstone with a thickness of approximately 1000 m are good seal beds (Fu Guang et al., 2001).

The Kela-2 gas field in the Kuqa Depression has been widely noticed since its discovery, because it is a large-sized dry gas field. As seen in Tables 1 and 2, the gases from the Kela-2 gas field are dominated by hydrocarbons, with the methane (C_1) contents of 97.08%−98.87%, the ethane (C_2) plus propane (C_3) contents of 0.04%−0.82%, normally without butane (C_4) and C_{5+} components. The gases are very dry, with the dryness index (C_1/C_{1-5}) of 0.992−0.999. The gases contain low CO_2 and N_2, within the range of 0.23%−0.94% and 0.04%−2.05%, respectively. The gases contain heavy methane and ethane carbon isotopic values ($\delta^{13}C_1$ and $\delta^{13}C_2$), within the range of -28.24‰− -26.16‰ and -19.40‰− -17.87‰. Normally, natural gases with these characteristics imply that they have a high maturity and originated from late-stage cracking of kerogen or coal at higher temperatures (Schoell, 1983; Dai Jinxing et al., 1992; Xu Yongchang et al., 1994).

Based on previous studies (Dai Jinxing et al., 2000; Jia Chengzhao et al., 2000; Li Jian et al., 2001; Liang Digang et al., 2002, 2003; Zhang Qiming, 2002; Li Xianqing, 2004; Li Xianqing et al., 2005, 2008), some particular geological and geochemical characteristics of natural gases in the Kela-2 gas field are summarized as follows.

(1) The Kela-2 gas field is obviously affected by ultra-high pressure, with its reservoir pressure of 67.74−75.94 MPa and the pressure factor up to 2.0−2.2.

Table 1 Chemical compositions of natural gases in the Kela-2 gas field of the Kuqa Depression*

Well	Depth (m)	Reservoir	C_1 (%)	C_2 (%)	C_3 (%)	iC_4 (%)	nC_4 (%)	C_{5+} (%)	CO_2 (%)	N_2 (%)	C_1/C_{1-5}
Kela 2	3499–3534.6	Lower Tertiary	98.05	0.40	nd	nd	nd	nd	0.94	0.61	0.996
Kela 2	3888–3895	Lower Cretaceous	98.22	0.50	0.04	0.01	0.01	0.01	0.61	0.60	0.994
Kela 2	3803–3809	Lower Cretaceous	98.08	0.42	0.04	0.01	0.01	nd	0.86	0.68	0.995
Kela 2	3937–3941	Lower Cretaceous	97.97	0.48	0.03	nd	nd	nd	0.87	0.65	0.995
Kela 201	3770–3795	Lower Cretaceous	98.87	0.69	nd	nd	nd	nd	0.40	0.04	0.993
Kela 201	3936–3938	Lower Cretaceous	97.08	0.05	nd	nd	nd	nd	0.82	2.05	0.999
Kela 203	3963–3975	Lower Cretaceous	97.59	0.80	0.02	nd	nd	nd	0.23	1.36	0.992
Kela 205	3789–3952	Lower Cretaceous	98.26	0.50	0.04	0.01	0.02	nd	0.72	0.45	0.994

Note: * After Li Xianqing et al., 2005. nd. Not detected or <detection limit.

Table 2 Isotope data of natural gases in the Kela-2 gas field*

Well	Depth (m)	Reservoir	$\delta^{13}C$ (‰, PDB)					
			C_1	C_2	C_3	iC_4	nC_4	CO_2
Kela 2	3499–3534.6	Lower Tertiary	-27.30	-19.40	-18.50	nd	-17.80	nd
Kela 2	3888–3895	Lower Cretaceous	-27.80	-19.00	nd	nd	nd	nd
Kela 2	3803–3809	Lower Cretaceous	-27.80	-18.70	nd	nd	nd	nd
Kela 201	3630–3640	Lower Cretaceous	-27.07	-18.48	-19.08	-19.44	-20.31	-19.78
Kela 201	3770–3795	Lower Cretaceous	-27.19	-17.87	-19.14	-19.25	-20.55	-22.75
Kela 201	3936–3938	Lower Cretaceous	-26.16	-18.09	-19.06	nd	-22.14	-15.83
Kela 201	4016–4021	Lower Cretaceous	-27.32	-19.00	-19.54	nd	-20.90	-18.58
Kela 202	1472–1481	Lower Tertiary	-28.24	-18.86	-19.15	nd	-20.91	-15.37

Note: * After Li Xianqing et al., 2005. nd. Not detected or <detection limit.

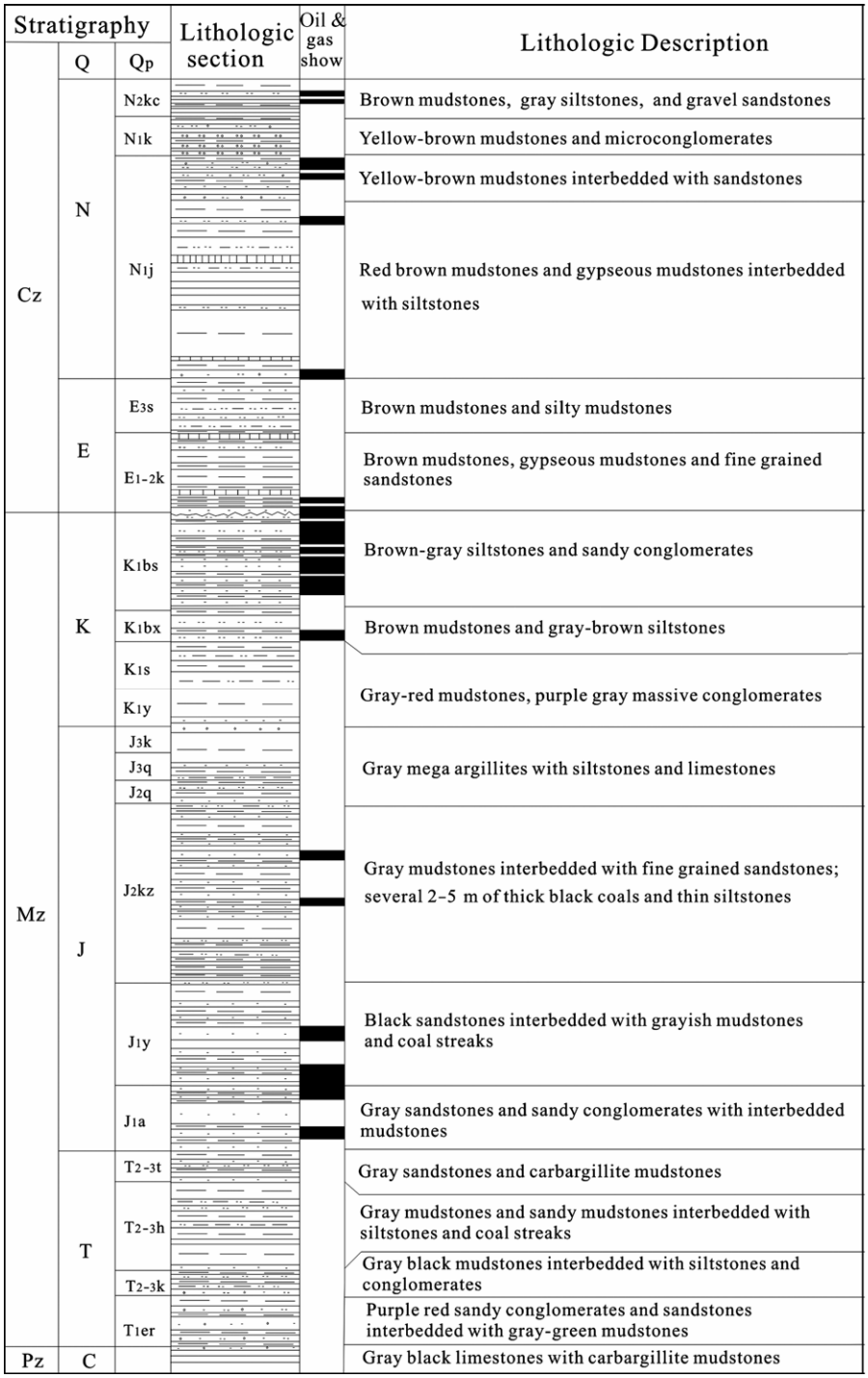

Fig. 2. Generalized stratigraphic column in the Kuqa Depression of the Tarim Basin.

(2) The Kela-2 gases feature very high methane contents (>97%), high dryness indices (C_1/C_{1-5}>0.99), and heavy carbon isotope ratios of methane and ethane ($\delta^{13}C_1$= -28.24‰− -26.16‰ and $\delta^{13}C_2$= -19.40‰− -17.87‰).

(3) The gypsum salt and gypsum-mudstone have the characteristics of high plasticity and large thickness (>400 m), which are the best regional cap rocks with the displacement pressure up to 60 MPa. The Eocene gypsum salt as a cap rock itself is an over-pressure bed with the same pressure factor as the reservoir. Therefore, the double preservative strata formed an excellent seal, which resulted in the preservation of the gas field.

(4) The foreland thrust faults played an important role in the formation and preservation of the natural gas field. The Kela-2 gas field is a fault-bend anticline structure in passive double tectonic layers on the Kelasu thrust structure belt. The foreland thrust faults not only control the structural pattern of fault-associated

folds, but also act as an important passage for the vertical migration of oil and gas.

(5) The structural traps were formed in the Kangcun Formation of the Neogene, and the migration passage of natural gases began to develop at 5.0 Ma. The Kela-2 trap was finally formed during the Kuqa stage (5.0–2.0 Ma). So it can be deduced that natural gases migrated only after trap formed, e.g. from 5.0 Ma to the present.

Previous studies on the Kela-2 gas field mainly put its focus on the characteristics of source rocks and the origin of natural gases (Qin Shengfei, 1999; Dai Jinxing et al., 2000; Li Jian et al., 2001; Zhao Mengjun et al., 2002; Zhang Qiming, 2002; Liang Digang et al., 2002, 2003; Li Xianqing et al., 2005). Some scholars thought that natural gases in the Kuqa Depression (including the Kela-2 gas field) were derived from the Jurassic coal-bearing strata, and are the typical coal-generating gases (Qin Shengfei, 1999; Dai Jinxing et al., 2000). Others deemed that the natural gases are related to both Jurassic and Triassic source rocks, and the contribution of the Jurassic coal-bearing source rocks to the gas generation is more than that of the Triassic source rocks (Li Jian et al., 2001; Zhao Mengjun et al., 2002; Liang Digang et al., 2002, 2003; Li Xianqing et al., 2005, 2008). The Kela-2 gases are dry and have heavy methane and ethane carbon isotopic values, for which no reasonable explanation has been provided so far. Further work is needed on the generation and accumulation processes of natural gases in the Kela-2 gas field by using the pyrolysis experimental and kinetic methods.

3 Methodology and experimental

The above information demonstrates that natural gases in the Kela-2 gas field are derived from the Triassic-Jurassic source rocks through the late-stage cracking of kerogen or coal. It is difficult to find low-mature source rocks with R_o values of less than 0.60% as the proper samples for pyrolysis experiments in the Kuqa Depression.

Three typical source rock samples were selected from the eastern part of the Kuqa Depression: a Jurassic coal sample, a Jurassic mudstone sample and a Triassic mudstone sample. The Jurassic coal sample (y-4) contains typical type-Ⅲ kerogen, with about 76% vitrinite, 7% exinite, 8% inertinite, and 9% semi-vitrinite plus semi-inertinite. In comparison with the Jurassic coal sample, two kerogen samples (y-6 and y-9) were separated from the Jurassic and Triassic mudstones using the procedures of Alpern (1980). Basic geochemical characteristics of the coal and kerogen samples are listed in Table 3.

Anhydrous pyrolysis experiments on coal and kerogen were conducted in gold tube reactors. Samples were loaded into gold tubes (6 mm o.d., 50 mm long), sealed and placed in stainless steel cells, then put into the pyrolysis furnace and kept at a confining pressure of 50 MPa during the entire experiment. The samples were heated to temperatures ranging from 300 to 600℃ at the heating rates of 2 and 20 ℃/h, respectively. When the required temperatures were reached, the cells were removed from the pyrolysed furnace. The gold tubes were used to make the following analyses.

In the C_1-C_5 gaseous hydrocarbon composition analysis, cleaned gold tubes were put in a vacuum system, and pierced with a needle. The gas products were released from the tubes and collected by a Toepler pump in order to be quantified. And then gas composition was determined on the HP5890 II gas chromatograph. Helium was used as the carrier gas. The temperature program used was isothermal for 2 minutes at 40℃, programmed at 30℃/min to 180℃, and then isothermal at 180℃ for 10 minutes. External standard method was applied to the quantification of gas components. The system has high sensitivity (it can analyze 0.01 mL volume of gas) and good accuracy (its standard deviation is less than 0.5%). After gas composition analysis, the residues of kerogen were dried, crushed, and then used for the measurement of vitrinite reflectance (R_o).

The GC-IRMS analysis was performed on a VG Isochrom II instrument. The GC was equipped with a Poraplot Quadax column (30 m in length, 0.32 mm in inner diameter) with the column head pressure of 8.9 Psi. The GC conditions are set as follows: the temperature program used was isothermal for 2 minutes at 40℃, programmed at 30℃/min to 150℃, and then held at 150℃ for 10 minutes. Reported carbon isotope data represented the arithmetic means of at least three duplicate analyses, and the repeatability was better than ±0.3‰. All carbon isotopic values were reported in per mil (‰) relative to the PDB standard.

The experimental data processing and the kinetic parameter calculation of methane generation were carried out with the KINETICS software (version 2.41) developed by Braun et al. (1987) and Burnham (1989). From previous studies (Tang et al., 1996), we used a discrete activation energy model to fit the experimental data for two different heating rates.

Based on the experimental data, the kinetic parameters for methane carbon isotope fractionation were calculated and fitted by the software GOR-Isotope (GeolsoChem Corporation, 2003). In kinetic modeling calculation of carbon isotope fractionation, methane was divided into two parts: ^{12}C-methane and ^{13}C-methane. These two parts were generated independently as two different matters with generation parameters for themselves. The method followed the same procedure published by Tang et al. (2000).

4 Results and discussion

4.1 The characteristics of methane yields and carbon isotopic ratios from pyrolysis experiments

As shown in Fig. 3, the cumulative methane yields are closely related to pyrolysis temperature and heating rate. In general, the cumulative methane yields of the Triassic and Jurassic source rocks increase with increasing pyrolysis temperature, even at different heating rates (20 and 2℃/h). The Jurassic coal and mudstone would generate more methane than the Triassic mudstone, especially at the high thermal evolution stage. For instance, at 20℃/h heating rate, when the pyrolysis temperature reaches 600℃, the Jurassic coal, Jurassic mudstone and Triassic mudstone can produce 173, 156 and 141 mL/g TOC cumulative methane, respectively. It is demonstrated that the Jurassic coal and mudstone have higher gas generation potential than the Triassic mudstone.

It is noted that there are a few differences in hydrocarbon-generating materials between coal and mudstone, although they are in the same coal-bearing strata. The organic petrological results (Li Xianqing, 2004) show that the Jurassic coal samples contain predominantly desmocollinite (70%) and a significant amount of exinite (7%), while the Jurassic mudstone contains less exinite (5%) and high inertinite (15%).

Shown in Fig. 4 is the variation of carbon isotopic ratios of cumulative methane, which was pyrolysed from the Jurassic and Triassic source rock samples in the Kuqa Depression. It is demonstrated that carbon isotopic ratios of methane pyrolyzed from the Jurassic coal and mudstone range from -37‰− -25‰, while those of methane from the Triassic mudstone are -39‰− -27‰. The carbon isotopic ratio of methane is correlated with pyrolysis temperature and heating rate. With increasing pyrolysis temperature, the carbon isotopic ratio of cumulative methane decreases at the low temperature stage (300−400℃), then increases gradually during the high temperature stage (400−600℃). The turning point (i.e., the lowest value) occurs at 400−420℃. There is a good positive correlation between the methane carbon isotope and pyrolysis temperature, after the pyrolysis temperature reaches 400−420℃.

The above variation trend of the methane carbon isotopic ratios is similar to that of coals and type-Ⅲ kerogens reported by Tang et al. (1996, 2000) and Lorant et al. (1998) in the confined system. It can also be compared with the general characteristics described by Berner et al. (1995) and Cramer et al. (1998, 2001) in the open system.

4.2 The kinetic parameters for methane generation and carbon isotope fractionation

The kinetic parameters for methane generation and carbon isotope fractionation based on the pyrolysis experiment data were calculated and fitted by the method described by Tang et al. (1996, 2000).

Shown in Fig. 5 are the kinetic parameters for methane generated from the Jurassic and Triassic source rocks in the Kuqa Depression, which were obtained by the kinetic modeling calculation of methane yields. Generally, the Jurassic-Triassic coal and mudstone in the Kuqa Depression have a wide activation energy distribution within the range of 180−289 kJ/mol. The ranges of activation energy distributions of methane generation in the Jurassic coal, Jurassic mudstone and Triassic mudstone are 197−268, 180−260 and 214−289 kJ/mol, respectively. The main peaks of activation energies of methane in the Jurassic coal, Jurassic mudstone and Triassic mudstone are 234, 205 and 264 kJ/mol, and their frequency ratios are 5.265×10^{13}, 9.761×10^{11}, and 2.270×10^{14} s^{-1}, respectively. All these parameters reflect the differences in methane generation in source rocks with different characteristics, even for the same type-Ⅲ organic matter.

Based on the kinetics of methane generation and experimental data for methane isotope fractionation of coal and kerogen samples at two different heating rates, the kinetic calculation of methane isotope fractionation can be fitted using the GOR-isotope software (GeolsoChem Corporation, 2003). There are a total of six parameters (Table 4). Detailed mathematic derivation and isotope fractionation constants were described in detail by Tang et al. (2000).

Table 3 Geochemical characteristics of coal and kerogen samples for pyrolysis experiment

Sample No.	Depth (m)	Age	Sample description	TOC (%)	R_o (%)	T_{max} (℃)	S_1 (mg/g)	S_2 (mg/g)	$\delta^{13}C$ (‰)
y-4	4316	J_2k	Coal	82.17	0.87	444	5.01	117.53	-23.83
y-6	4400	J_1y	Kerogen from dark mudstone	79.78	0.89	448	10.78	100.48	-23.96
y-9	4958	T_{3t}	Kerogen from dark mudstone	61.69	0.98	460	2.08	64.75	-24.40

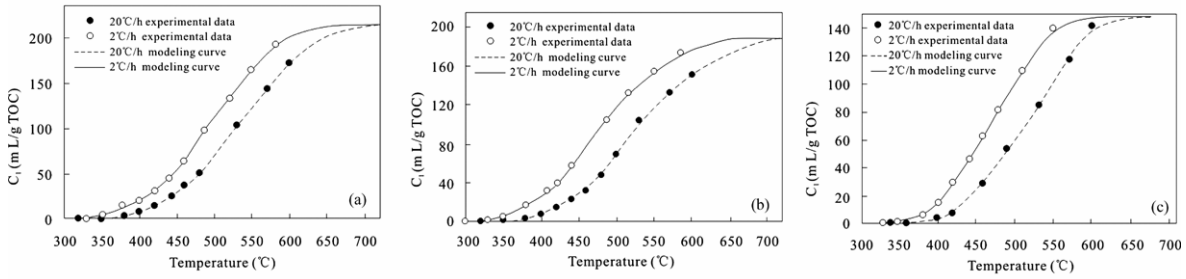

Fig. 3. The cumulative methane (C_1) yields pyrolyzed from source rock samples in the Kuqa Depression and their kinetic calculations. (a) Jurassic coal; (b) Jurassic mudstone; (c) Triassic mudstone.

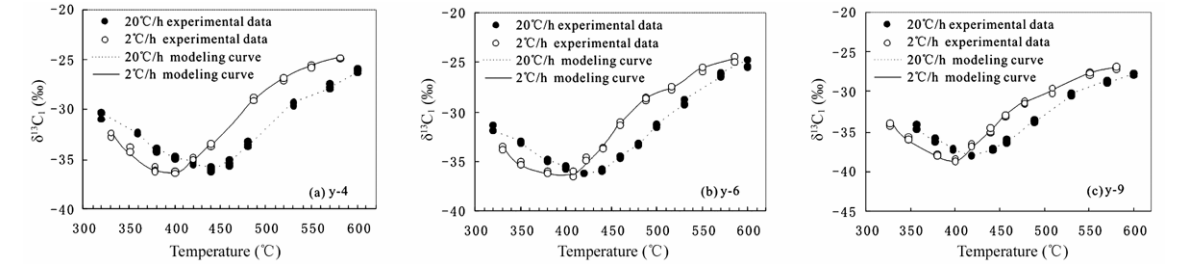

Fig. 4. The carbon isotopic ratios of methane pyrolyzed from source rock samples in the Kuqa Depression and their kinetic calculations. (a) Jurassic coal; (b) Jurassic mudstone; (c) Triassic mudstone.

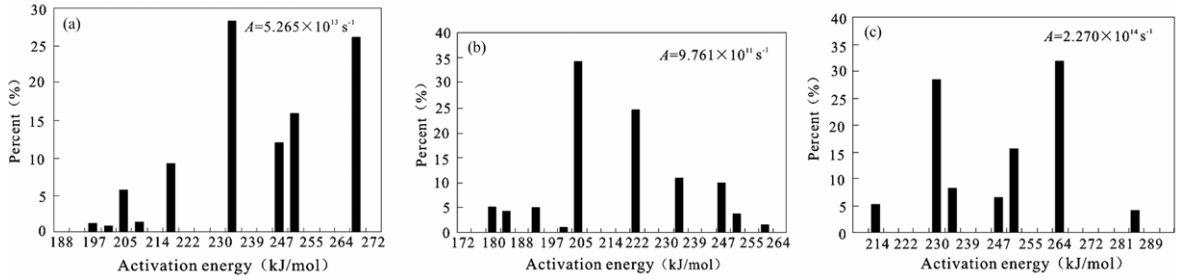

Fig. 5. Activation energy and frequency factor of methane generation of source rock samples in the Kuqa Depression. (a) Jurassic coal; (b) Jurassic mudstone; (c) Triassic mudstone.

The results of activation energy distributions for ^{12}C-methane and ^{13}C-methane generated from the Jurassic and Triassic source rocks in the Kuqa Depression are illustrated in Fig. 6. There are some differences in activation energies and frequency factors for ^{12}C-methane and ^{13}C-methane in the Jurassic coal, Jurassic mudstone and Triassic mudstone. Both ^{12}C-methane and ^{13}C-methane in the Jurassic coal have a range of variations between 201 and 293 kJ/mol in activation energy, with their frequency factors of 1.000×10^{15} and 1.020×10^{15} s^{-1}, respectively. The activation energies of ^{12}C-methane and ^{13}C-methane in the Jurassic mudstone are 176−255 and 176−255 kJ/mol, with their frequency factors of 1.000×10^{12} and 1.020×10^{12} s^{-1}. The activation energy range and frequency factor of ^{12}C-methane in the Triassic mudstone are 209−280 kJ/mol and 1.000×10^{14} s^{-1}, while those of ^{13}C-methane are 209−280 kJ/mol and 1.020×10^{14} s^{-1}, respeictively. All these reflected the differences for ^{12}C-methane and ^{13}C-methane generation in different source rocks.

The kinetics parameters for methane carbon isotope fractionation were obtained (Table 4). The average activation energies of methane carbon isotope fractionation in the Jurassic coal, Jurassic mudstone and Triassic mudstone are 227.9, 204.8 and 230.6 kJ/mol, respectively. Their activation thresholds are 0.01094, 0.01094 and 0.01090. The above differences in kinetic parameters between these samples can influence the geological modelling results of methane generation and carbon isotope fractionation.

4.3 Generation kinetics model of the Kela-2 gases

According to the burial and thermal evolution histories (Liang Digang et al., 2002), the kinetic modeling calculation of the Jurassic and Triassic source rocks from the center of the Baicheng Sag and Well Kela-2 in the Kuqa Depression has been carried out, and the results are shown in Figs. 7–9.

Table 4 Methane carbon isotope fractionation kinetics parameters for the studied source rocks

Sample No.	Methane carbon isotope fractionation kinetics parameter*					
	α	β_L (J/mol)	β_H (J/mol)	Eo (kJ/mol)	σ (J/mol)	γ
y-4	1.020	137.66	322.14	227.9	32.74	0.01094
y-6	1.020	117.98	247.52	204.8	22.86	0.01094
y-9	1.020	109.19	204.19	230.6	11.60	0.01090

Note: * After Tang et al., 2000. α. Isotope fractionation factor; β_L. lowest activation energy difference; β_H. highest activation energy difference; Eo. average activation energy; σ. variance; γ. activation energy threshold.

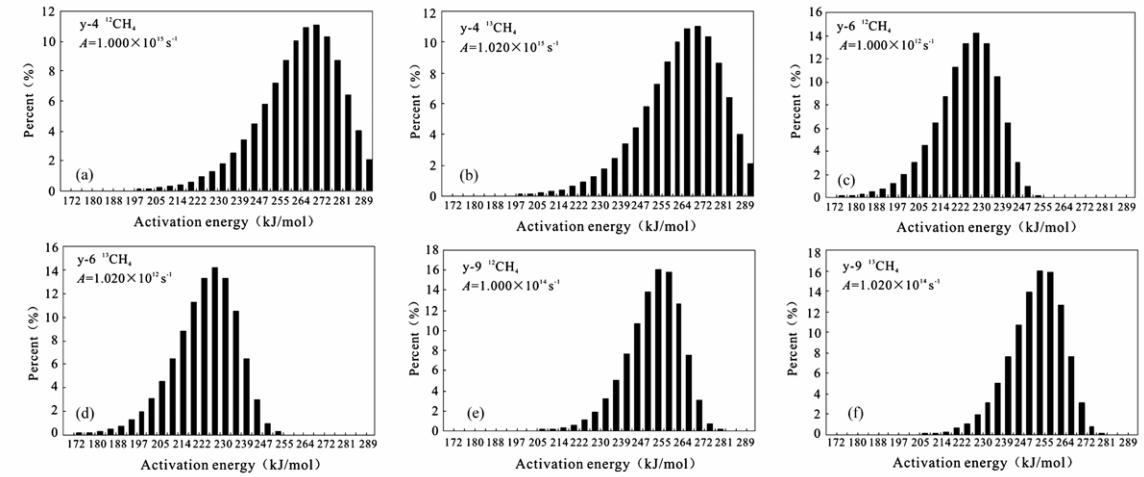

Fig. 6. The activation energy distributions of ^{12}C-methane (a, c, e) and ^{13}C-methane (b, d, f) generated from source rock samples in the Kuqa Depression. (a, b) Jurassic coal; (c, d) Jurassic mudstone; (e, f) Triassic mudstone.

4.3.1 Source of the Kela-2 gases

As shown in Figs. 7 and 8, during the Middle Jurassic period, the carbon isotope ratio of methane derived from the Jurassic coal and coal-associated mudstone in Well Kela-2 and the center of the Baicheng Sag predominately occurred after 5.0 Ma, and became much heavier than ever, both reaching about -26‰. The Kela-2 gases have methane carbon isotopic ratios of -28.24‰− -26.16‰. It can be inferred that both Jurassic coal and Jurassic mudstone in Well Kela-2 or in the center of the Baicheng Sag have similar methane carbon isotope modeling results, which are consistent with the present methane carbon isotope ratios of the Kela-2 gases. Thus, the Jurassic coal and mudstone can be regarded as the main gas source rocks of the Kela-2 gas field, with its gas source area including Well Kela-2 and the center of the Baicheng Sag. This viewpoint was supported by the relevant research work (Dai Jinxing et al., 2000; Li Jian et al., 2001; Liang Digang et al., 2002, 2003).

The results of carbon isotope modeling of methane generation for Triassic mudstone from Well Kela-2 and the center of the Baicheng Sag are shown in Figs. 9 and 10. According to the methane carbon isotopic ratios of Kela-2 gases, it can be concluded that the charge time of gas from the base of the Middle-Upper Triassic in Well Kela-2 and the center of the Baicheng Sag should start at 13–4 Ma. Of course, this gas charge model inferred from the methane carbon isotope kinetic modeling does not match with the formation time of trap-migration faults in the Kela-2 gas field. It is suggested that the Triassic mudstone made a minor contribution to the Kela-2 gas field.

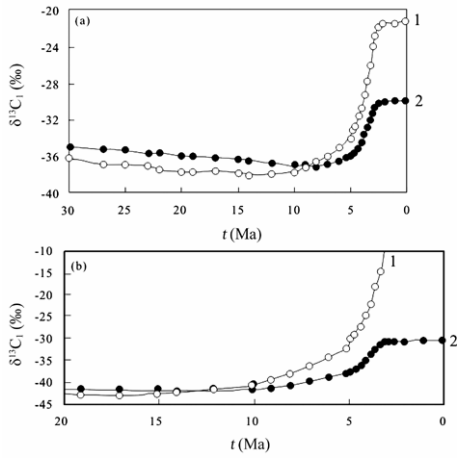

Fig. 7. The kinetic calculation of methane carbon isotope fractionation from the Jurassic source rocks in Well Kela-2. (a) Jurassic coal; (b) Jurassic mudstone. 1. Instantaneous $\delta^{13}C_1$; 2. cumulative $\delta^{13}C_1$.

According to previous research results (Jia Chengzhao et al., 2000; Liang Digang et al., 2002), the Jurassic coal-bearing mudstone is 467 m in thick-

ness and corresponds to that of the Triassic mudstone (489 m) at the Kapusalianghe profile near Well Kela-2. However, the organic carbon content of the Jurassic mudstone (about 1.75% TOC on average) is obviously higher than that of the Triassic mudstone (only 0.89% TOC on average). The total gas yield of source rocks from pyrolysis experiment (Li Xianqing, 2004) demonstrates that the Jurassic coal and mudstone (173 and 156 mL/g TOC, respectively) produced more methane than the Triassic mudstone (141 mL/g TOC). The sedimentary facies studies (Tarim Oilfield Company, 2003) showed that the Jurassic dark mudstone is distributed extensively with the coverage greater than that of the Triassic strata. Thus, the total gas yield generated from the Jurassic coal-bearing source rocks is higher than that of the Triassic source rocks. In addition, in terms of the gas generation and trap formation history, it can be seen that the time of gas generation from the Triassic source rocks is much earlier than the time of trap formation. So, it would cause large amounts of natural gases to be lost, and then to be accumulated. From the generation and accumulation history of natural gases, it is considered that the gas contribution of the Jurassic coal-bearing source rocks in the Kela-2 gas field is obviously higher than that of the Triassic source rocks. These facts also proved the above conclusion that gas sources were from the Kela-2 gas field.

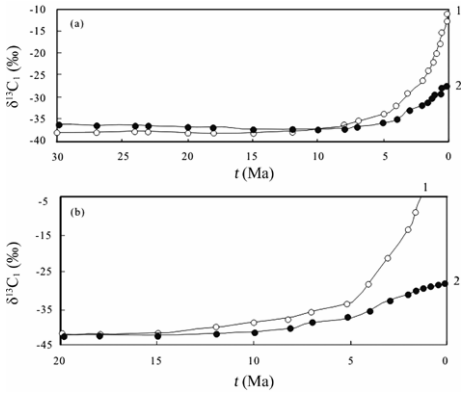

Fig. 8. The kinetic calculation of methane carbon isotope fractionation from the Jurassic source rocks in the center of the Baicheng Sag. (a) Jurassic coal; (b) Jurassic mudstone. 1. Instantaneous $\delta^{13}C_1$; 2. cumulative $\delta^{13}C_1$.

4.3.2 Maturity of the Kela-2 gases

Take the base of the Lower and Middle Jurassic source rocks in Well Kela-2 and the center of the Baicheng Sag (i.e., gas source kitchen of Kela-2 gas field) for example. The modeling results of methane carbon isotope fractionation from the Jurassic coal and mudstone in Well Kela-2 and the center of the Baicheng Sag are shown in Figs. 11 and 12. It is demonstrated that the carbon isotopic ratio of instantaneous methane is obviously heavier than that of cumulative methane, which is from the Jurassic coal and mudstone with R_o >1.3%.

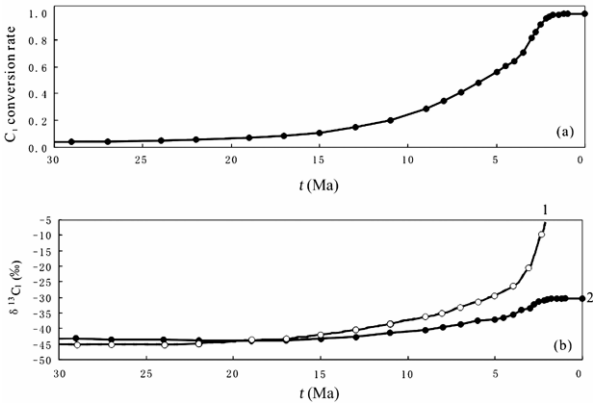

Fig. 9. The kinetic calculation of methane generation and carbon isotope fractionation from the Triassic mudstone in Well kela-2. 1. Instantaneous $\delta^{13}C_1$; 2. cumulative $\delta^{13}C_1$.

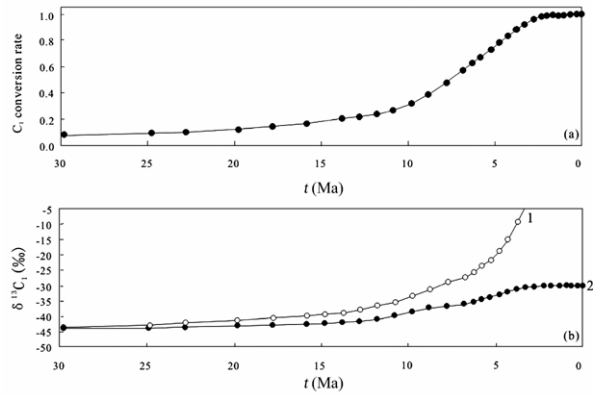

Fig. 10. The kinetic calculation of methane generation and carbon isotope fractionation from the triassic mudstone in the center of the baicheng sag. 1. instantaneous $\delta^{13}C_1$; 2. cumulative $\delta^{13}C_1$.

On the basis of the relationship between methane carbon isotopic value and R_o, the maturity range of natural gases in the Kela-2 gas field was further evaluated. Listed in Tables 3 and 4, methane carbon isotopic ratios of the Kela-2 gases are mainly -28‰– -26‰, and about -27‰ on average. Considering the uplift and erosion at 2.0 Ma, the gas field formation at 1.0 Ma, and the increasing R_o (0.50%–0.56%) after 1.0 Ma, the gas maturity of the Kela-2 gas field has been identified as follows. The calculated gas maturity of the Kela-2 gas field shows that R_o values of the Jurassic coal and Jurassic mudstone are 1.6%–2.5% and 1.3%–2.5%, respectively. Therefore, it is suggested that the Kela-2 gases belong to the staged cumulative gases, which were obviously accumulated in the late stage. This indicates that the maturity of the Kela-2 gases lies between 1.3% and 2.5%.

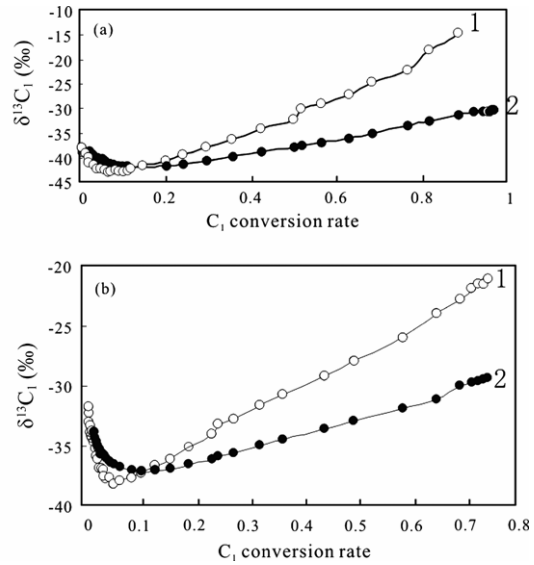

Fig. 11. Relationship between methane carbon isotope fractionation and methane (C_1) conversion in Well Kela-2. (a) Jurassic coal; (b) Jurassic mudstone. 1. Instantaneous $\delta^{13}C_1$; 2. cumulative $\delta^{13}C_1$.

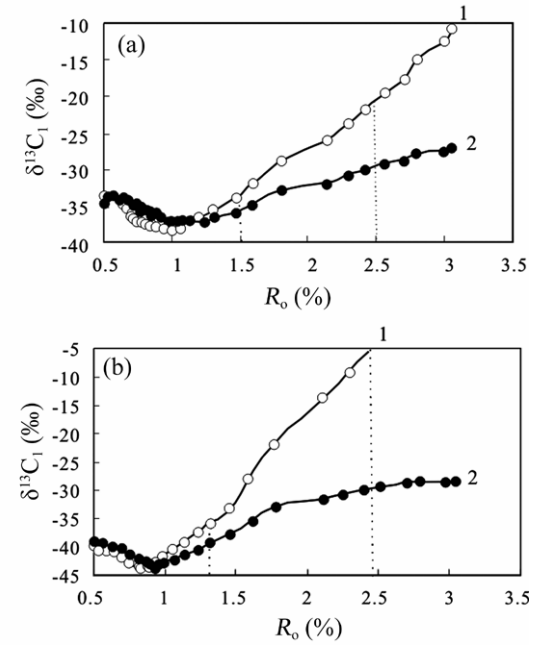

Fig. 12. Relationship between methane carbon isotope fractionation and R_o in the centre of the Baicheng Sag. (a). Jurassic coal; (b) Jurassic mudstone; 1. Instantaneous $\delta^{13}C_1$; 2. cumulative $\delta^{13}C_1$.

4.3.3 Accumulation time of the Kela-2 gases

By considering the Lower-Middle Jurassic coal measures as the main effective gas source rocks in the Kuqa Depression, gas accumulation time of the Kela-2 gas field was deduced from methane generation and carbon isotope fractionation kinetics. The charging and accumulation of natural gases for the Lower-Middle Jurassic coal occurred after 5.0 Ma (Li Xianqing, 2004)，corresponding to the stratum temperature of 180−240℃ and R_o of 1.5%−2.5%, respectively. The gas charging and accumulation for the Lower-Middle Jurassic mudstone occurred at 5.0−0 Ma, corresponding to the stratum temperature of 160−240℃ and R_o of 1.3%−2.5%, respectively. Therefore, the Kela-2 gases were primarily accumulated after 5.0 Ma.

4.3.4 The generation model of the Kela-2 gases

Based on the formation model of natural gases in the Kelasu tectonic belt (Liang Digang et al., 2002) and in combination with the above characteristics of methane carbon isotope kinetics, the model of generation and accumulation of natural gases in the Kela-2 gas field has been further complemented and modified (Fig. 13). This model not only reduces the deficiency of the formation model of natural gases, which traditionally depends on the matching relationship among source rock, reservoir, cap rock, and trap, but also is a useful reference in the study of other gas fields in the Tarim Basin.

5 Conclusions

The Kela-2 gas field, discovered in the Kuqa Depression of the Tarim Basin, belongs to an ultra-high pressure gas field (pressure factor up to 2.0−2.2). The Kela-2 gases are typical dry gases, which contain more than 97% methane, with the dryness index being more than 0.99. The carbon isotopic ratios of methane and ethane range from -28.24‰ to -26.16‰, and from -19.40‰ to -17.87‰, respectively. The results of pyrolysis experiments show that the Jurassic coal and Jurassic mudstone (173 and 156 mL/g TOC) have more gas yields than the Triassic mudstone (141 mL/g TOC). It can be seen that source rocks from the Jurassic coal-bearing strata have higher gas generating potential than the Triassic strata.

The kinetic parameters of methane generation for the Triassic-Jurassic source rocks were calculated by using the KINETICS software. The activation energies of methane generated from the Jurassic coal, Jurassic mudstone and Triassic mudstone are (197−268) kJ/mol, (180−260) kJ/mol, and (214−289) kJ/mol, respectively. Their main peaks of activation energies are 234, 205, and 264 kJ/mol, and their frequency factor ratios are 5.265×10^{13}, 9.766×10^{11}, and 2.270×10^{14} s^{-1}.

The kinetic parameters of methane carbon isotope fractionation were obtained through the GOR-Isotopic software. The average activation energies of methane carbon isotope fractionation of the Jurassic coal, Jurassic mudstone and Triassic mudstone are 227.9, 204.8, and 230.6 kJ/mol, respectively. Their activation energy thresholds are 0.01094, 0.01094, and 0.01090, respectively.

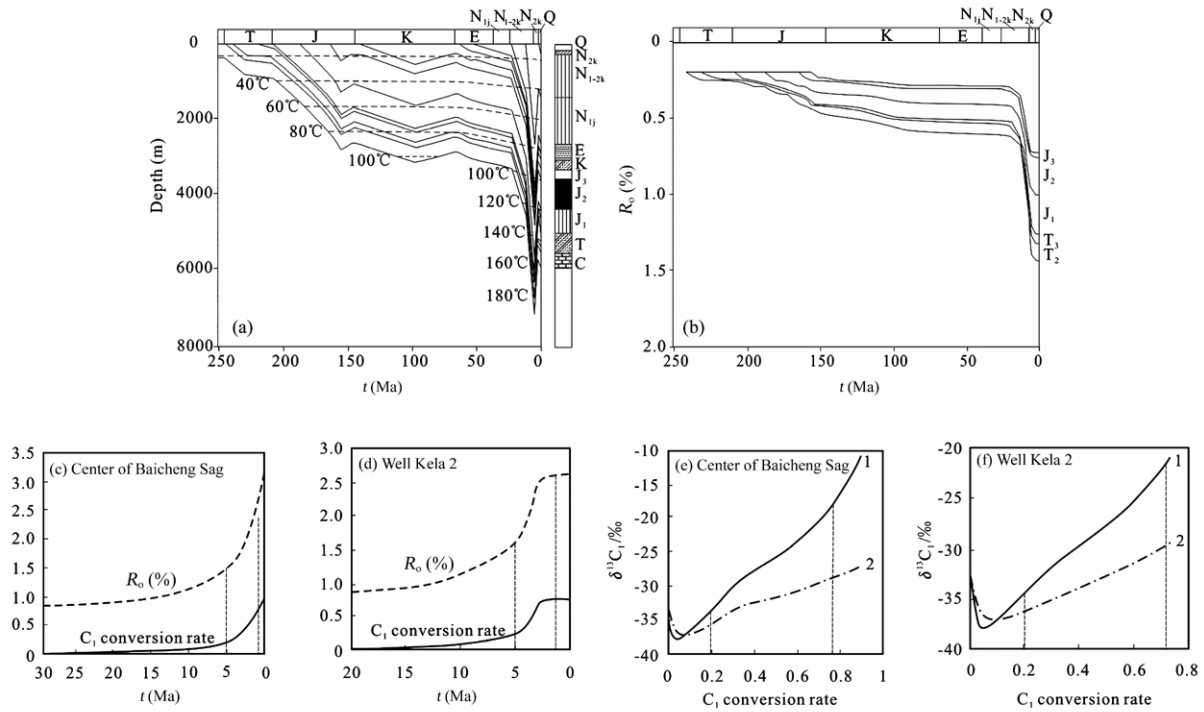

Fig. 13. The generation model of natural gases in the Kela-2 gas field. 1. Instantaneous $\delta^{13}C_1$; 2. cumulative $\delta^{13}C_1$; (a) Burial history; (b) R_o evolutionary history for the center of the Baicheng Sag; (c) hydrocarbon generation history; (d) carbon isotope evolution of Well Kela-2: (e) hydrocarbon generating history; (f) carbon isotope evolution.

In combination with the geological background, the source, maturity, and accumulation time of the Kela-2 gases were further discussed in terms of the kinetic modeling results of gas generation and methane carbon isotope fractionation. The Kela-2 gases were mainly derived from the Middle and Lower Jurassic source rocks, belonging to the staged cumulative gases. The Kela 2 gases were chiefly accumulated during the last 5.0 Ma, and the R_o values of the source rocks range from 1.3% to 2.5%. On the basis of this research, a kinetic model of natural gas generation and accumulation in the Kela-2 gas field is established. This kind of study provides the insights and methods for the quantitative assessment and dynamic research on natural gases.

Acknowledgements We would like to thank the Tarim Oilfield Company for its technical support and sampling. This research work was financially supported jointly by the National Large-sized Oil and Gas Fields Science and Technology Research Program (Grant Nos. 2011ZX05007-002 and 2011ZX05033-004), the National Key Foundational Research and Development "973"Project (Grant No. 2012CB 214702), the Fundamental Research Funds for the Central Universities (Grant No. 2010YM01), the Earmarked Fund of the State Key Laboratory of Organic Geochemistry, Guangzhou Institute of Geochemistry, Chinese Academy of Sciences (Grant No. OGL-200808), the Research Project of State Key Laboratory of Coal Resources and Safe Mining, China University of Mining and Technology (Grant No. SKLCRSM10B04), and the New-century Excellent Talent Program of Ministry of Education (Grant No. NCET-06-0204). The authors are extremely grateful to Prof. Peng Ping'an, Prof. Liang Digang, and Prof. Wang Zhaoming for their strong support. We highly appreciate discussions with Prof. Wang Feiyu and Dr. Hu Guoyi who made good suggestions. Special thanks are due to Dr. Lu Hong, Dr. Liu Dayong and Dr. Shuai Yanhua for giving much help in information collection, experimental analysis and data processing.

References

Alpern B. (1980) The petrology of kerogen. In *Kerogen* (ed. Durand B.) [M]. pp.284−321. Technip, Paris.

Behar F., Kressmann S., and Vandenbroucke M. (1991) Experimental simulation in a confined systems and kinetic modeling of kerogen and oil cracking [J]. *Org. Geochem.* **19**, 173−189.

Behar F., Vandenbroucke M., and Tang Y. (1997) Thermal cracking of kerogen in open and closed systems: Determination of kinetic parameters and stoichiometric coefficients for oil and gas generation [J]. *Org. Geochem.* **26**, 321−339.

Berner U., Faber E., and Stahl W. (1992) Mathematical simulation of the carbon isotopic fractionation between huminitic coals and related methane [J]. *Chem. Geol.* **94**, 315−319.

Berner U., Faber E., Scheeder G., and Panten D. (1995) Primary cracking of algal and land plant kerogens: kinetic modeling of kerogen and oil cracking [J]. *Organic Geochemistry*. **126**, 233−245.

Braun R.L. and Burnham A.K. (1987) Analysis of chemical reaction kinetics using a distribution of activation energies and simple models [J]. *Energy & Fuels*. **1**, 153−161.

Burnham A.K. (1989) A simple kinetic model of petroleum formation and cracking [P]. Lawrence Livermore Lab. Report UCID21665, March.

Clayton C. (1991) Carbon isotope fractionation during natural gas generation from kerogen [J]. *Mar. Pet. Geol.* **8**, 232−240.

Cramer B., Krooss B. M., and Littke R. (1998) Modelling isotope fractionation during primary cracking of natural gas: A reaction kinetic approach [J]. *Chem. Geol.* **149**, 235−250.

Cramer B., Faber E., Gerling P., and Krooss B.M. (2001) Reaction kinetics of stable carbon isotopes in natural gas-insights from dry, open system pyrolysis experiments [J]. *Energy & Fuels*. **15**, 517−532.

Dai Jinxing and Qi Houfa (1989) The $\delta^{13}C$-R_o relationship of coal-derived hydrocarbon gases in China [J]. *Chinese Science Bulletin*. **34**, 690−692 (in Chinese).

Dai Jinxing, Pei Xigu, and Qi Houfa (1992) *The Geology of Natural Gas in China* [M]. pp.56−170. Petroleum Industry Press, Beijing (in Chinese).

Dai Jinxing, Zhong Ningning, Liu Dehan, Xia Xinyu, Yang Jianye, and Tang Dazhen (2000) *Geological Base and Control Factor of Giant and Medium-sized Coal-derived Gas Fields in China* [M]. pp.191−230. Science Press, Beijing (in Chinese).

Liang Digang, Zhang Shuichang, Chen Jianping, Wang Feiyu, and Wang Peirong (2003) Organic geochemistry of oil and gas in the Kuqa Depression, Tarim Basin, NW China [J]. *Organic Geochemistry*. **34**, 873−888.

Faber E. (1987) Zur Isotopengeochemie gasförmiger Kohlenwasserstoffe [J]. *Erdöl Erdgas & Kohle*. **103**, 210−218.

Fu Guang, Wang Pengyan, and Fu Xiaofei (2001) Seal characteristics of Eocene mudstone cap rock in Kuche depression and its importance in controlling accumulation of oil and gas [J]. *Geological Journal of China Universities*. **7**, 477−482 (in Chinese with English abstract).

Galimov E.M. (1988) Sources and mechanisms of formation of gaseous hydrocarbons in sedimentary rocks [J]. *Chem. Geol.* **71**, 77−96.

GeolsoChem Corporation (2003) GOR-Isotope. Version 1. pp.48.

Gu Jiayu, Jia Jinhua, and Fang Hui (2002) The characteristics of reservoirs in Tarim Basin and the origin of high porosity and penetrability reservoirs [J]. *Chinese Science Bulletin*. **47**, 9−15.

Jenden P.D., Drazan D.J., and Kaplan I.R. (1993) Mixing of thermogenic natural gases in northern Appalachian basin [J]. *A.A.P.G. Bull.* **77**, 980−998.

Jia Chengzhao, Qin Shengfei, and Li Qiming (2000) Formation and distribution of coal-formed petroleum in the Kuqa foreland depression of Tarim Basin. In *International Symposium on Hydrocarbon from Coal* (eds. Dai Jinxing, Fu Chengde, and Xia Xinyu) [M]. pp.176−190. Petroleum Industry Press, Beijing (in Chinese).

Li Jian, Xie Zhengye, Li Zhisheng, Luo Xia, Hu Guoyi, and Gong Se (2001) The study on natural gas sources in the Kuqa depression, Tarim Basin [J]. *Petroleum Exploration and Development*. **28**, 29−33 (in Chinese with English abstract).

Li Xianqing, Hou Dujie, Tang Youjun, Hu Guoyi, and Xiong Bo (2003) Molecular geochemical evidence for the origin of natural gases from dissolved hydrocarbons in the Ordovician Formation in central Ordos Basin [J]. *Chinese Journal of Geochemistry*. **22**, 193−202.

Li Xianqing (2004) *Research and Application of Hydrocarbon Generation Kinetics of Natural Gas* [D]. pp.4−108. Research report of postdoctoral work. Guangzhou Institute of Geochemistry, Chinese Academy of Sciences, Guangzhou (in Chinese).

Li Xianqing, Hou Dujie, Hu Guoyi, and Li Jian (2005) *The Characteristics of Fluids and the Formation of Natural Gases in the Central Gas Field in the Ordos Basin* [M]. pp.86−132. Geological Publishing House, Beijing (in Chinese).

Li Xianqing, Hu Guoyi, Li Jian, Hou Dujie, Dong Peng, Song Zhihong, and Yang Yunfeng (2008) The characteristics and sources of natural gases from Ordovician weathered crust reservoirs in the Central Gas Field in the Ordos Basin [J]. *Chin. J. Geochem.* **27**, 109−120.

Li Xianqing, Xiao Xianming, Tang Yongchun, Xiao Zhongyao, Mi Jingkui, Liu Dehan, Shen Jiagui, and Liu Jingzhong (2004) The generation and accumulation of natural gas from Yinan 2 gas pool in Kuqa Depression [J]. *Chinese Science Bulletin.* **49**, 107−114.

Li Xianqing, Xiao Xianming, Tang Yongchun, and Tian Hui (2008) The modeling of carbon isotope kinetics and its application to the evaluation of natural gas [J]. *Frontiers of Earth Science in China*. **2**, 96−104.

Li Xianqing, Xiao Zhongyao, Hu Guoyi, Tian Hui, and Zhou Qiang (2005) Origin and geochemistry of natural gas in Kuqa Depression, Tarim Basin [J]. *Xinjiang Petroleum Geology.* **26**, 489−492 (in Chinese with English abstract).

Liang Digang, Zhang Shuichang, Chen Jianping, Wang Peirong, and Wang Feiyu (2002) Geochemistry of hydrocarbon in Kuqa Depression, Tarim Basin. In *New Advances on Organic Geochemistry* (eds. Liang Digang, Huang Difan, Ma Xinhua, and Li Jingming) [M]. pp.22−42. Petroleum Industry Press, Beijing (in Chinese).

Lorant F. and Prinzhofer A. (1998) Carbon isotopic and molecular constraints on the formation and the expulsion of thermogenic hydrocarbon gases [J]. *Chem. Geol.* **147**, 249−264.

Prinzhofer A.A. and Huc A.Y. (1995) Genetic and post-genetic molecular and isotopic fractionations in natural gases [J]. *Chem. Geol.* **126**, 281−290.

Prinzhofer A.A. and Pernaton E. (1997) Isotopically light methane in natural gas: Bacterial imprint or diffusive fractionation [J]. *Chem. Geol*. **142**, 193−200.

Qin Shengfei (1999) The origin of abnormal natural gas in the Kuqa Depression, Tarim Basin [J]. *China Petroleum Exploration*. **4**, 21−23 (in Chinese with English abstract).

Rooney M.A., Claypool G.E., and Chung H.M. (1995) Modelling thermogenic gas generation using carbon isotope ratios of natural gas hydrocarbons [J]. *Chem. Geol*. **126**, 219−232.

Schoell M. (1980) The hydrogen and carbon isotopic composition of methane from natural gases of various origins [J]. *Geochim. et Cosmochim. Acta.* **44**, 649−661.

Schoell M. (1983) Genetic characterization of natural gases [J]. *A.A.P.G. Bull.* **67**, 2225−2238.

Shen Ping, Shen Qixiang, Wang Xianbin, and Xu Yongchang (1988) Characteristics of isotope composition of gas form hydrocarbon and identification of coal-type gas [J]. *Sci. Sin.* (Ser. B). **31**, 734−747.

Stahl W. and Carey B.D. (1975) Source-rock identification by isotope analyses of natural gases from fields in the Val Verde and Delaware basins, West Texas [J]. *Chem. Geol.* **16**, 257−267.

Stahl W. (1977) Carbon and nitrogen isotopes in hydrocarbon research and exploration [J]. *Chem. Geol*. **20**, 121−149.

Tang Y., Jenden P.D., Nigrini A., and Teerman S.C. (1996) Modeling early methane generation in coal [J]. *Energy and Fuels*. **10**, 659−671.

Tang Y., Perry J.K., Jenden P.D., and Schoell M. (2000) Mathematical modeling of stable carbon isotope ratios in natural gases [J]. *Geochim. et Cosmochim. Acta*. **64**, 2673−2687.

Whiticar M.J. (1994) Correlation of natural gases with their sources. In *The Petroleum System—From Source to Trap* (eds. Magoon L.B. and Dow W.G.) [C]. *A.A.P.G. Memoir*. **50**, 261−283.

Xu Yongchang, Shen Ping, Liu Wenhui, Chen Jianfa, and Tao Mingxin (1994) *The Genetic Theory of Natural Gas and Its Application* [M]. pp.182−356. Science Press, Beijing (in Chinese).

Zhang Qiming (2002) Deep overpressure gas accumulation [J]. *Chinese Science Bulletin*. **47** (supp.), 78−84.

Zhao Mengjun, Lu Shuangfang, and Li Jian (2002) The geochemical features of natural gas in the Kuqa Depression and the discussion on the gas source [J]. *Petroleum Exploration and Development.* **29**, 4−7 (in Chinese with English abstract).